ELSEVIER

Polymer 43 (2002) 1069–1080

polymer

www.elsevier.com/locate/polymer

Comparative DSC kinetics of the reaction of DGEBA with aromatic diamines. II. Isothermal kinetic study of the reaction of DGEBA with *m*-phenylene diamine

V.L. Zvetkov*

Central Laboratory of Physical Chemical Mechanics, Bulgarian Academy of Sciences, Acad. G. Bontchev str., Ibl., 1113 Sofia, Bulgaria

Received 11 July 2001; received in revised form 3 October 2001; accepted 14 October 2001

Abstract

In the first part of the present series the non-isothermal kinetics of the reaction of an epoxy resin based on diglycidyl ether of bis-phenol A (DGEBA) with *m*-phenylene diamine (*m*PDA) was studied. A four step kinetic analysis was applied using differential scanning calorimetry (DSC) data. It allowed us to confirm the validity of the three molecular autocatalytic model of this reaction, as well as to obtain reliable kinetic data in programmed temperature mode.

The isothermal study of the DGEBA–*m*PDA reaction was performed applying a similar kinetic approach: (i) analysis at the peak maximum of the DSC curves; (ii) apparent activation energy analysis of the isothermal DSC data; (iii) integral and differential curve fitting methods; and (iv) modeling of the reaction and comparison of the model with the experiment.

It was established that the overall kinetic parameters measured under programmed temperature conditions sufficiently well described the isothermal shift of the DSC curves along the logarithmic time scale, especially the initial stage of the reaction. A more precise analysis of the data showed that the isothermal DSC kinetics obeyed a formal model whose power exponent was approximately 2.5, or it was not well represented by the mechanistic-like three molecular autocatalytic velocity equation. Nevertheless, the activation energy of the autocatalytic rate constant determined at constant temperature mode, i.e. $E_{a,i} = 50.67$ kJ mol^{-1}, was found out in close agreement with the one obtained previously in programmed temperature mode, $E_{a,n} = 50.50$ kJ mol^{-1}. On the contrary, the ratio of the impurity catalytic to autocatalytic rate constant was slightly temperature dependent.

Keywords: Epoxy–amine reaction; Isothermal differential scanning calorimetry; Autocatalytic kinetics

1. Introduction

The results derived from the reaction kinetics of different epoxy–diamine systems are directly applicable in the processing. The differential scanning calorimetry (DSC) technique has two important advantages: (i) it is the only reaction rate method that permits to measure with a great accuracy both the rate of reaction and the degree of conversion; (ii) the DSC cell may be considered as a mini-reactor with a vanishing temperature gradient. Therefore, the DSC kinetics provides the variables required for solution of the heat/mass transfer equations, namely: the heat flow (proportional to the rate of reaction) and the heat generation (proportional to the degree of conversion).

The epoxy–aromatic diamine formulations are of a practical importance since the cured thermosets on their basis are rigid, high T_g polymer networks. The reaction kinetics of diglycidyl ether of bis-phenol A (DGEBA) with *m*-phenylene diamine (*m*PDA) has more theoretical than practical significance, although the mixture of diaminodiphenyl methane (DDM) with *m*PDA is a commercial epoxy hardener suitable for different industrial applications.

The epoxy–amine reactions are usually depicted by the scheme of Horie et al. [1], viz.

$$RNH_2 + Ep + EpOH \xrightarrow{k_1} RR'NH + EpOH \quad (1a)$$

$$RNH_2 + Ep + R_iOH \xrightarrow{k_1'} RR'NH + R_iOH \quad (1b)$$

$$RR'NH + Ep + EpOH \xrightarrow{k_2} RR'R''N + EpOH \quad (1c)$$

$$RR'NH + Ep + R_iOH \xrightarrow{k_2'} RR'R''N + R_iOH \quad (1d)$$

where RNH_2, $RR'NH$, and $RR'R''N$ represent the primary, secondary, and tertiary amines; Ep is the epoxy; EpOH and R_iOH are the catalytic hydroxyl containing species which

* Tel.: +359-2-979-3905; fax: +359-2-703-433.
E-mail address: zvetval@bgcict.acad.bg (V.L. Zvetkov).

0032-3861/02/$ - see front matter
PII: S0032-3861(01)00695-4

are accumulated during the reaction or are present as impurities; both R' and R'' express an additional formation of EpOH link and simultaneous consumption of a primary or secondary amine, correspondingly; k_i and k'_i ($i = 1, 2$) are Arrhenius type rate constants; k_1 and k_2 refer to the autocatalytic reaction path, whereas k'_1 and k'_2 relate to the impurity-catalyzed reaction.

The scheme (1) is based on a certain mechanism, first proposed by Smith [2], postulating that the rate determining step overcomes through an epoxy–amine–hydroxyl complex formation in transition state.

Two mathematical descriptions of the epoxy–amine reactions according to the above scheme are found in the literature. The first one is expressed by a part of the following system of ordinary differential equations [3–5]:

$$-\frac{de}{dt} = (k'_1 c_0 + k_1 x) e (a_p + r' a_s) \tag{2a}$$

$$-\frac{da_p}{dt} = (k'_1 c_0 + k_1 x) e a_p \tag{2b}$$

$$-\frac{da_s}{dt} = (k'_1 c_0 + k_1 x) e (r' a_s - a_p) \tag{2c}$$

$$\frac{da_t}{dt} = (k'_1 c_0 + k_1 x) e r' a_s \tag{2d}$$

$$\frac{dx}{dt} = (k'_1 c_0 + k_1 x) e (a_p + r' a_s) \tag{2e}$$

where e, x, c_0, a_p, a_s, and a_t are the epoxy, the product (hydroxyl groups), the initial hydroxyl impurity, the primary, secondary, and tertiary amine group concentrations, respectively; $r' = k_2/k_1 = k'_2/k'_1$ is the reactivity ratio of the secondary to primary amines.

The scheme of Horie et al. may be described with another set of differential equations [6]:

$$-\frac{de}{dt} = k_{1h}(OH) e (a_1 + r a_2) \tag{3a}$$

$$-\frac{da_1}{dt} = 2 k_{1h}(OH) e a_1 \tag{3b}$$

$$-\frac{da_2}{dt} = k_{1h}(OH) e (r a_2 - a_1) \tag{3c}$$

where $r = k_{2h}/k_{1h}$ is the secondary to primary amine hydrogen reactivity ratio; a_1 and a_2 are the primary and secondary amine hydrogen concentrations; (OH) is the total concentration of the catalytic hydroxyl containing species generated during the reaction and initially presented as impurities; the subscript 'h' denotes hydrogen atom formalism.

A brief comparative analysis of Eqs. (2a–e) and (3a–c) is given below.

1. The first set of differential equations allows to extract solutions (analytical or numerical) with respect to the concentration of either the reactants or the products. Consequently, it is preferable to use when a competitive (or subsequent) side reaction takes place [7,8].
2. The mass balance equations according to Eqs. (2a–e) and (3a–c) differ, viz.

$$a_p + a_s + a_t = a'_0, \qquad \text{and} \qquad 2a_p + a_s = 2a'_0 - x$$

$$a_1 + 2a_2 + 2a_t = a_0, \qquad \text{and} \qquad a_1 + a_2 = a_0 - x$$

where $x = (e_0 - e)$ and $a_t = (x - a_s)/2 = (x - a_2)/2$ in the both cases; e_0, a'_0, and a_0 are the initial molar concentrations of the epoxy, the amine groups, and the amine hydrogen atoms, respectively.
3. The definition of the secondary to primary amine reactivity ratios, according to Eqs. (2a–e) and (3a–c), is also different. $r' = k_2/k_1 = 1/2$ infers that the primary amine groups (having two hydrogen atoms) are twice more reactive compared to the secondary ones (having one hydrogen atom). Conversely, the ideal value of r is unity. The factor 2 in Eq. (3b) accounts for the fact that a reacted primary amine hydrogen automatically converts the remaining hydrogen into secondary one. Hence, the elemental rate constant representing the primary amine reaction incorporated in Eqs. (3a–c) is doubled compared to that in Eqs. (2a–e) or $k_{1h} = 2k_1$, whereas $k_{2h} = k_2$.

The assumptions $r' = k_2/k_1 = 1/2$ and $R_0 = 2a'_0/e_0 = 1$ (or $r = k_{2h}/k_{1h} = 1$ and $R_0 = a_0/e_0 = 1$) lead to the well-known dimensionless velocity equation that is usually referred to as Horie et al. overall model, viz.

$$\frac{d\alpha}{dt} = (K' + K\alpha)(1 - \alpha)^2 = K(B + \alpha)(1 - \alpha)^2 \tag{4}$$

where $\alpha = x/e_0$ is the degree of conversion; $R_0 = 1$ represents the equimolar initial amine to epoxy ratio; $K = k_1 e_0^2/2$; and $K' = k'_1 e_0 c_0/2$ (or $K = k_{1h} e_0^2$; and $K' = k'_{1h} e_0 c_0$) are dimensionless rate constants whose expression depends on the mass balance principle accepted.

In the previous work of the series, we have performed a kinetic study of the reaction of a low molecular epoxy resin based on DGEBA with *m*PDA under programmed temperature conditions [9]. The kinetic parameters of the autocatalytic rate constant K (the activation energy and the pre-exponential factor, E_a and K_0, respectively) have been determined. It has been established that the value of E_a corresponds satisfactorily to the literature data [10–13]. The accuracy test of the kinetic parameters in programmed temperature mode has shown a perfect agreement between the model and the experiment, having in mind that the parameter B was supposed to be a constant.

As is aforementioned, the DSC is the only direct reaction rate technique that can validate Eq. (4) in isothermal mode from the plot of the reduced reaction rate, $\dot{r}$, versus α, viz.

$$\dot{r} = \frac{d\alpha}{dt}\frac{1}{(1 - \alpha)^2} = K' + K\alpha \tag{5}$$

The analysis of the literature data concerning the reaction kinetics of DGEBA with *m*PDA has indicated inconstancy with respect to the value of the power exponent which is observed to agree with [11,12] or to differ from the theoretical value [10,13]. The deviation from the overall three molecular velocity equation will be further discussed based on some simplifications accepted in the above-described kinetic model. This is the first aim of the present work.

The second aim of the study consists in accuracy test of the kinetic parameters measured under programmed temperature conditions in isothermal mode, and vice versa. The advantages and disadvantages of the formal representation of the velocity equation will be also considered.

2. Experimental

2.1. Sample preparation

The epoxy resin (a low molecular homologue of DGEBA under the trade name DER-332 of Dow Chemical, with epoxy equivalent of 174 kg kmol^{-1}) and the amine hardener (*m*PDA, 99% purity grade) were supplied by Fluka and applied as received. Stoichiometric amounts of the two components were melted at 343 K, undercooled at 328 K, and thoroughly mixed in a high speed stirrer. After degassing under vacuum the samples were prepared for future use and kept in refrigerator as proposed by Gillham et al. [14,15]. Their experimental procedure for measuring the fractional conversion was also accepted. Fresh reactive mixtures were weekly prepared.

2.2. Experimental technique

The experimental method used in this study was DSC. A Perkin–Elmer DSC-2C instrument, equipped with subambient accessory (intercooler II) and interfaced to 3600 Data Station with the isothermal or standard data acquisition and analytical software, was applied as experimental technique. The cooling device was needed since both the enthalpy and the onset glass transition temperature, T_g, were simultaneously measured. The calibration was regularly made using In and Zn standards at each scanning rate being used. Special attention to the slope of the baseline was paid. At the end of each scanning experiment the *Y*-value at the final temperature, T_f, was tested and, if necessary, adjusted to a constant value.

The ultimate reaction enthalpy, ΔH_0 (normalizing parameter of the reaction rate), the jump of the specific heat capacity of the monomer mixture, ΔC_{p0}, the onset T_{g0}, and the corresponding glass transition parameters of the fully reacted specimens, $T_{g\infty}$ and $\Delta C_{p\infty}$, were determined in scanning mode and were previously reported [9]. $\Delta T_g = -4.5$ K was used as onset T_g correction at $dT/dt = 0$, i.e. under isothermal condition.

The T_g versus α data were obtained at 373 K by heating the samples in the DSC instrument for different periods of time. The samples were rapidly cooled at 80 K min^{-1} and subsequently scanned at 10 K min^{-1} from $T_s = 223$ K to $T_f = 568$ K. Both the residual heat, ΔH_r, and the current T_g values were measured from the second scans. The fractional conversion was quantitatively calculated as: $\alpha = 1 - \Delta H_r/\Delta H_0$ [12,14,15].

It has to be mentioned that partially cured DGEBA–*m*PDA samples began to react during devitrification if α exceeded approximately 0.5. Fig. 1 shows the measurement of ΔH_r in these cases. It also infers the importance of the baseline control in scanning mode.

The isothermal runs were performed in the temperature range from 353 to 403 K in 10 K increment. The sample pans were inserted into the sample holder at 303 K and, after the instrument equilibration, heated to the desired curing temperature, T_c, at 40 K min^{-1}. The heat changes were acquired until no detectable deviation from the final baseline was observed and the total reaction enthalpy, ΔH_t, was determined at each T_c. The residual enthalpy, ΔH_r, and the glass transition temperature of the cured samples, T_{gf}, were measured after eliminating the aging peak by heating the samples 10 K above the corresponding T_c. Then, the samples were rapidly cooled to 253 K at 80 K min^{-1} and the second scans were recorded at $dT/dt = 10$ K min^{-1}.

The experimental data used in the further analysis were intermediate files (with respect to the time at the peak maximum) of at least three runs performed at each T_c. Since the values of ΔH_t were twice more scattered than those of ΔH_r (up to $\alpha_f \leq 0.93$), the differential and integral data were normalized according to the equations

$$\frac{d\alpha}{dt} = \frac{d\Delta H}{\Delta H_0\, dt}\,\frac{\Delta H_0 - \Delta H_r}{\Delta H_t}; \qquad \text{and} \qquad \alpha = \frac{\Delta H}{\Delta H_0}\,\frac{\Delta H_0 - \Delta H_r}{\Delta H_t} \tag{6}$$

where ΔH is the enthalpy evolution that changes from 0 to ΔH_t.

The experiments above 393 K exhibited significant

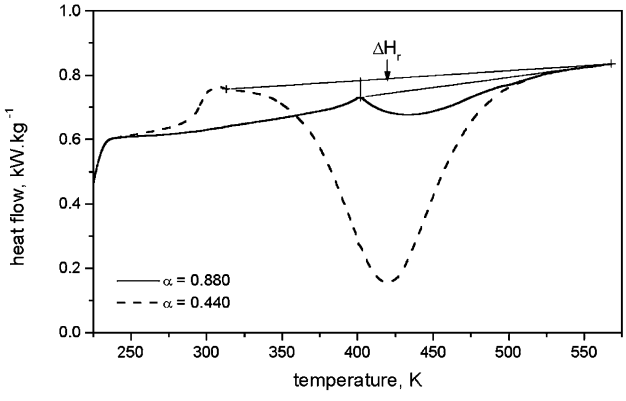

Fig. 1. Experimental measurement of the residual reaction enthalpy at high degrees of conversion.

reaction advance during the instrument equilibration. A detectable conversion at the beginning of the isothermal runs at 383 K ($\alpha_0 = 0.015$) was also established, whereas $\alpha_0 = 0.005$ at 373 K was found using extrapolation. It has to be also mentioned that T_c were not the actual values. Since both ΔH_r and onset T_g were measured from the second scans at 10 K min^{-1}, the instrument was calibrated at this heating rate. The typical temperature correction of our sample holder at zero heating rate is $\Delta T = 1.3$ K. Then, the actual T_c values, $T_c = T_{c,i} + 1.3$ K, will be further presented.

2.3. Analytical methods

The original experimental data were collected in a Perkin–Elmer 3600 Data station and the data files were transferred into an IBM compatible personal computer (DX2-486, DOS 6.2). The further analysis was performed with the aid of a self-developed software. A detail description of the program was reported in Ref. [9].

3. Results and discussion

One of the aims of the study consists in accuracy test of the kinetic parameters obtained under programmed temperature conditions [9]. The isothermal DSC kinetics of the reaction between DGEBA and *m*PDA has been considered in several works [10–13] but the data of Sourour and Kamal [11] seem to be the most appropriate ones for this purpose. These authors have concluded that their experimental data obeyed sufficiently well the overall model of Horie et al. Moreover, the epoxy equivalent of the resin they used was exactly the same as that applied in our studies, i.e. 174 kg kmol^{-1}.

The values of the calculated rate constants in the investigated temperature range are shown in Table 1. A test of the kinetic parameters is graphically represented in Fig. 2. The time scale of the curves is calculated from the analytical solution of Eq. (4) [9], viz.

$$Kt = g(\alpha) = \frac{1}{1+B}\frac{\alpha}{1-\alpha} + \frac{1}{(1+B)^2}\ln\frac{B+\alpha}{B(1-a)} \qquad (7)$$

The two sets of kinetic parameters give comparable results

Table 1
Comparison of the isothermal curves calculated using the kinetic data of Sourour and Kamal [11] with those predicted following the velocity equation evaluated in programmed temperature mode [9]

Rate constants	Temperature (K)				Ref.
	353	383	393	403	
$K \times 10^3$ (s^{-1})	1.157	4.136	6.058	8.705	[11]
$K' \times 10^5$ (s^{-1})	0.875	7.647	14.64	27.13	
$B = K'/K$	0.0076	0.0185	0.0242	0.0312	
$K \times 10^3$ (s^{-1})	1.055	4.059	6.077	8.917	[9]
$K' \times 10^5$ (s^{-1})	2.636	10.15	15.19	22.29	
$B = K'/K$	0.025	0.025	0.025	0.025	

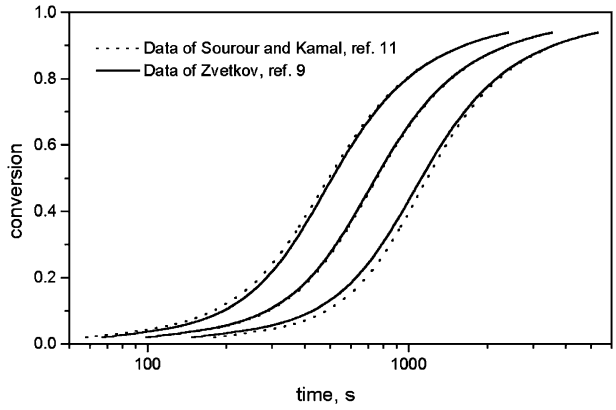

Fig. 2. Comparison of the kinetic data obtained following the model of Horie et al. in isothermal [11] and programmed temperature [9] mode.

within the temperature range of 393 ± 20 K. The disagreement apart from this range is probably due to the different temperature dependency of the parameter B, as the data in Table 1 indicate. The evaluated velocity equation of Sourour and Kamal [11] predicts an extremely low ratio of the two rate constants at lower T_c, e.g. $B = 0.0076$ at 353 K. Other authors have found that B should exceed at least 0.015 for several formulations based on epoxy resins whose epoxy equivalent, 174.3 kg kmol^{-1} [6,16], was nearly the same as the aforementioned value. In our opinion, the increase of K' against T_c should be considerably less, as is later commented.

The further kinetic analysis of the reaction of DGEBA with *m*PDA is performed following four subsequent steps. Each of them is discussed in a separate subsection.

3.1. Kinetic analysis at the peak maximum

The isothermal DSC curves, normalized according to Eq. (6), and the corresponding integral curves obtained in the temperature range from 354.5 to 384.5 K are shown in Figs. 3 and 4, respectively. The overall parameters which characterize the isothermal reaction of DGEBA with *m*PDA at the beginning, $t = 0$, at the maximum of the DSC curves, $t = t_p$, and at the end of the experiments, $t = t_f$, are summarized in Table 2. $(d\alpha/dt)_0$ and $(d\alpha/dt)_p$ are the reaction rates at $t = 0$ and $t = t_p$, α_p and α_f are the degrees of conversion at $t = t_p$ and $t = t_f$, correspondingly. T_{gf} is the final glass transition temperature extrapolated at zero heating rate.

The first step of our kinetic approach requires a quantitative estimate of the power exponent, n, of the 'general' velocity equation of the form

$$\frac{d\alpha}{dt} = (K' + K\alpha)(1-\alpha)^n = K(B+\alpha)(1-\alpha)^n \qquad (8)$$

The parameters n and B are calculated according to the following algebraic system:

$$B = \frac{1-(n+1)\alpha_p}{n};$$
$$B = \frac{\alpha_p(1-\alpha_p)^n}{(d\alpha/dt)_p/(d\alpha/dt)_0 - (1-\alpha_p)^n} \qquad (9)$$

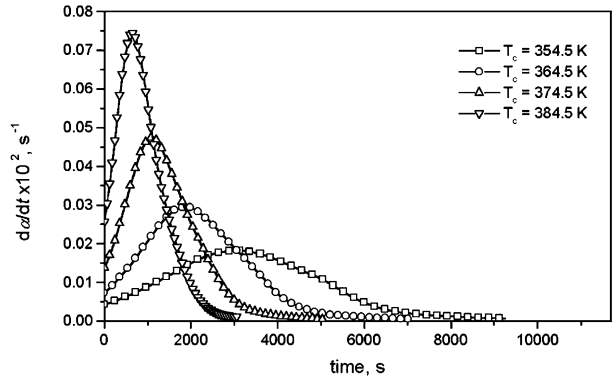

Fig. 3. Normalized original DSC curves of DGEBA–*m*PDA reaction obtained at different curing temperatures.

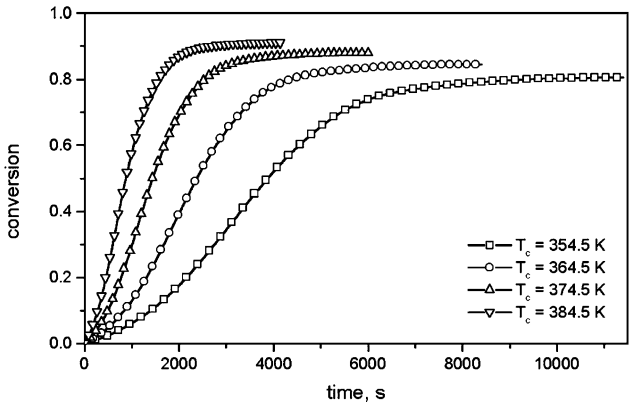

Fig. 4. Normalized integral DSC curves of DGEBA–*m*PDA reaction obtained at different curing temperatures.

The first expression arises from the boundary condition at $t = t_p$, where $d^2\alpha/dt^2 = 0$ and $\alpha = \alpha_p$. The second one appears from the relation $(d\alpha/dt)_p/(d\alpha/dt)_0$ rearranged against the parameter B. Therefore, Eqs. (9) represent the straight line between two points of the reduced reaction rate, at $\alpha = 0$ and $\alpha = \alpha_p$, respectively. Table 3 shows the values of n and B (or B' if $\alpha_0 > 0$ [9]) iteratively calculated according to Eqs. (9).

The estimate of n in Table 3 infers a principal difference between the non-isothermal and isothermal kinetics of DGEBA–*m*PDA reaction that will be later commented in more detail. It is evident that the experimental data obey a velocity equation whose overall order in the investigated temperature range seems to be 2.5 rather than 3.

On the other hand, the values of B and α_p confirm the suggestion that the partially converted fractions during instrument equilibration become detectable at $T_c \geq 374.5$ K. Then, the original curves must be corrected for the initial degree of conversion, α_0, as pointed out in Section 2. The elapsed time, t_0, has to be also added. The actual B and α_p values are measured subsequently from the α_0-corrected curves applying the procedure described in the preceding paper [9]. All these parameters, viz. α_0, t_0, B, and α_p, are given in Table 3.

Although the experimental data obtained at 394.5 and 404.5 K seem to be reliable they are not presented here since the overall reaction order sharply increases. This finding has a certain explanation but it will not be discussed in this study.

3.2. Apparent activation energy analysis of the differential scanning calorimetry data

There are several methods found in the literature to estimate quantitatively the apparent activation energy of the epoxy–amine reactions:

1. The logarithmic plot of the reaction rate at a given degree of conversion (or at a characteristic event), e.g. $(d\alpha/dt)_{0.5}$, $(d\alpha/dt)_p$, $(d\alpha/dt)_{gel}$, versus reciprocal temperature [11].
2. The logarithmic plot of the time to reach a given degree of conversion (or a characteristic event), e.g. $t_{0.5}$, t_p, t_{gel}, t_v, versus reciprocal temperature [10–13].
3. The superposition of the fractional conversion versus log(time) curves and subsequent Arrhenius plot of the shift factor [14–16].
4. The superposition of the glass transition temperature versus log(time) curves and subsequent Arrhenius plot of the shift factor [14–16].

The first three methods are directly applied in the present work, whereas the premise that there is one-to-one relationship between T_g and α [14] is tested at 374.5 K only. All three types of kinetic analysis are carried out using both the original and α_0-corrected data.

The Arrhenius dependencies of characteristic ordinate and abscissa variables, $(d\alpha/dt)_{0.5}$ and t_p, are shown in Figs. 5 and 6, respectively.

The plot of $\log(d\alpha/dt)_{0.5}$ versus $1/T_c$ is slightly altered

Table 2
Integral characteristics of the DGEBA–*m*PDA reaction

T_c[a] (K)	$(d\alpha/dt)_0 \times 10^3$ (s^{-1})	$(d\alpha/dt)_p \times 10^3$ (s^{-1})	α_p	t_p (s)	T_{gf}[b] (K)	α_f	t_f
354.5	0.0426	0.1820	0.3555	3054	357.5	0.805	11,400
364.5	0.0737	0.2946	0.3555	1866	371.5	0.845	8,400
374.5	0.1376	0.4733	0.3505	1110	382.5	0.880	6,000
384.5	0.2560	0.7435	0.3390	648	393.0	0.910	4,200

[a] The actual values of T_c are determined at $dT/dt = 0$, viz. $T_c = T_{c,i} + 1.3$ K.
[b] The actual values of T_{gf} are determined at $dT/dt = 0$, viz. $T_{gf} = T_{gf,m} - 4.5$ K.

Table 3
Calculation of the parameters n and B (or B') according to Eq. (9) and all related data

T_c (K)	n	B (B')[a]	α_0	t_0 (s)	α_p[b]	B[b]
354.5	1.61	0.0465	–	–	0.3555	0.0465
364.5	1.59	0.0505	–	–	0.3555	0.0505
374.5	1.59	0.0595	0.005	40	0.3530	0.0550
384.5	1.60	0.0735	0.015	67	0.3510	0.0580

[a] B' is calculated from the original curves—see Ref. [9].
[b] α_p and B are measured from the α_0-corrected curves.

(within the error limits) by the α_0-correction. The E_{ap} value derived from the data in Fig. 5, $E_{ap} = 52.3 \pm 0.4$ kJ mol^{-1}, perfectly agrees with E_{ap} obtained in programmed temperature mode [9]. Another differential plot, $\log(d\alpha/dt)_p$ versus $1/T_c$, exhibits a similar trend.

Fig. 6 represents the plot of $\ln(t_p)$ versus $1/T_c$ of the original and α_0-corrected data. It yields: $E_{ap} = 58.5 \pm 1.8$ kJ mol^{-1} and $E_{ap} = 54.8 \pm 0.6$ kJ mol^{-1}, respectively. As one can establish, the second estimate of E_{ap} is far more reliable.

A semi-logarithmic plot of α versus log(time), suitable for superposition of the data into a master curve, is demonstrated in Fig. 7. The shift factor against $T_c = 364.5$ K, $A_T = [\ln(t_{364.5}) - \ln(t_T)]$, and the E_{ap} values determined using both the original and α_0-corrected data are given in Table 4. The E_{ap} estimate calculated from the second set of data is of the same magnitude as the aforementioned values: $E_{ap} = 53.5 \pm 0.1$ kJ mol^{-1}. It quantitatively confirms the assumption that the decrease of α_p at $T_c \geq 374.5$ K is probably due to the partially converted fraction at the beginning of the experimental observations.

Following the statement of Gillham et al. [14,15] that one-to-one relationship between T_g and α exists, a master T_g versus log(time) curve at $T_c = 374.5$ K is obtained. It is shown in Fig. 8. The theoretical curves in the investigated temperature range, which are presented in the same figure, are calculated using the well-known semi-empirical formula

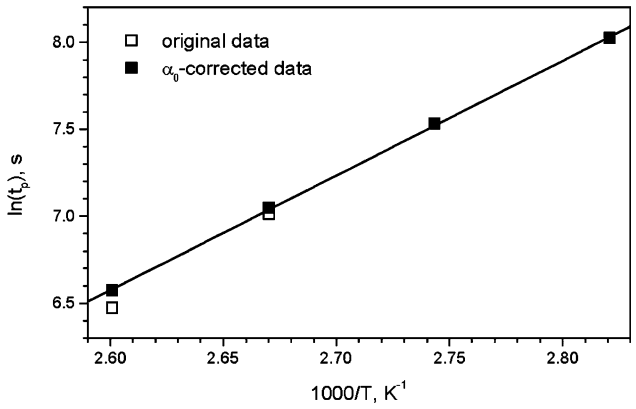

Fig. 6. Arrhenius plot of the time for reaching the peak maximum of DGEBA–*m*PDA reaction.

of DiBenedetto [17], viz.

$$\frac{T_g - T_{g0}}{T_{g0}} = \frac{(E_\alpha/E_m - F_\alpha/F_m)\alpha}{1 - (1 - F_\alpha/F_m)\alpha} = \frac{(a_E - b_F)\alpha}{1 - (1 - b_F)\alpha} \quad (10)$$

where $a_E = E_\alpha/E_m$ is the ratio of the lattice energies of crosslinked and uncrosslinked species and $b_F = F_\alpha/F_m$ is the corresponding ratio of their segmental mobilities.

If the above ratios are supposed to be constants, that does not seem an exactly reasonable hypothesis [18], they might be derived applying non-linear regression. Taking into account the onset T_g at zero heating rate, that has been previously reported: $T_{g0} = 248$ K [9], the best fit values of the coefficients in DiBenedetto formula have been determined, namely: $a_E = 0.575$ and $b_F = 0.33$.

Fig. 8 also shows the test of the theoretical time to vitrify, t_v, at 374.5 K. It is defined as the time where T_g calculated according to Eq. (10) reaches T_c. The experimental onset T_g measured from a subsequent scan whose $t_f = t_v$ is well comparable with the theoretically predicted one.

The plot of $\ln(t_v)$ versus $1/T_c$ yields: $E_{ap} = 54.2 \pm 1.0$ kJ mol^{-1}. It is consistent with the result obtained from the plot of $\ln(t_p)$ versus $1/T_c$.

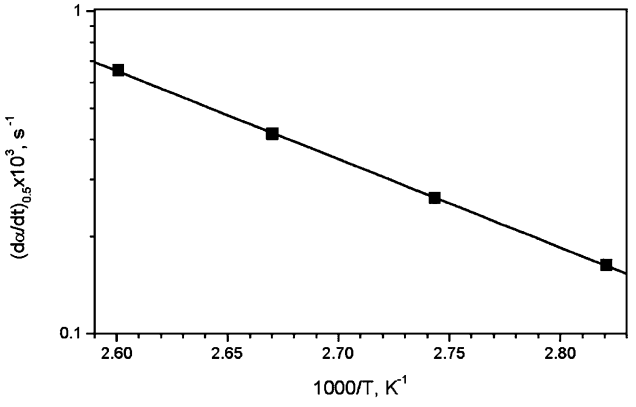

Fig. 5. Arrhenius plot of the rate at 50% conversion of DGEBA–*m*PDA reaction.

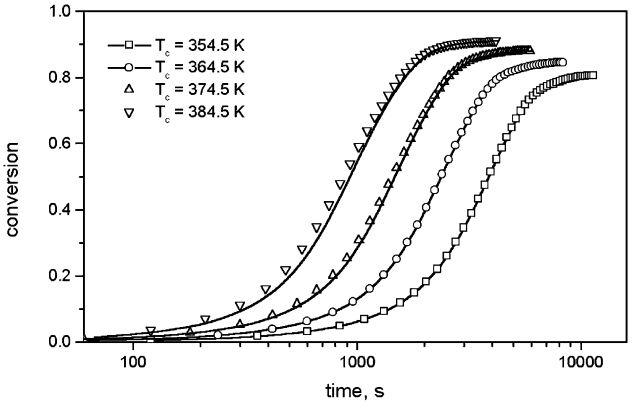

Fig. 7. Superposition plot of the degree of conversion versus log(time) scale of DGEBA–*m*PDA reaction.

Table 4
The E_{ap} values calculated according to the conversion versus ln (time) shift method

$A_T = [\ln(t_{364.5}) - \ln(t_T)]$, data type	Temperature (K)				E_{ap} (kJ mol^{-1})
	354.5	364.5	374.5	384.5	
Original data	−0.4953	0	0.5132	1.0314	57.7 ± 1.4
α_0-corrected data	−0.4953	0	0.4715	0.9201	53.5 ± 0.1

All apparent activation energy data are summarized in Table 5.

We have to point out that the apparent methods are strictly operative when a single rate constant controls the chemical reaction. If it does not happen, then an increase of E_{ap} regarding the fractional conversion indicates a competitive rate controlling path (or a competitive mechanism) whose E_a must be higher. The agreement between the non-isothermal and all isothermal E_{ap} values measured using α_0-corrected data implies that the autocatalytic mechanism seems to predominate.

The comparison of the results in Fig. 2 confirms this suggestion. According to our kinetic data [9], E_a of the autocatalytic rate constant is higher than that obtained by Sourour and Kamal [11]. Conversely, the superposition of the two sets of simulated curves exhibits an opposite trend.

3.3. Single DSC curve kinetic analysis

The DSC kinetic analysis of the epoxy-amine reactions has been mainly performed using the rearranged form of Eq. (8), viz.

$$\dot{r} = \frac{d\alpha}{dt}\frac{1}{(1-\alpha)^n} = K' + K\alpha = K(B+\alpha) \qquad (11)$$

The variable $\dot{r}$ is a characteristic expression of the autocatalytic reactions known as reduced reaction rate. The adjustable power exponent n has been found to vary as a rule within the range of $1 \le n \le 2$. It has been often observed that $n < 2$ [10,13,19–23] even when the epoxy–amine reactions of model compounds have been studied [19,20]. If $n = 2$, then Eqs. (11) and (5) become identical, which means that the experiment exactly obeys the overall model of Horie et al.

Some of the cited authors have tried to clarify the discrepancy of n from the theoretical value. Attempts have been made to explain the case $n = 1$ [3,22] assuming a stepwise formation of the transition state complex and responding transfer of the rate determining step. A square root power exponent regarding the amine component, or $n = 1.5$, has been accepted, as well [19,21–23]. Unfortunately, the mechanistic sense of the lower value of n has not been still described and it is more probably a result of other reasons. This fact infers that the investigation in these cases lies on a formal basis. Nevertheless, the formal kinetics has certain practical importance, as is later discussed.

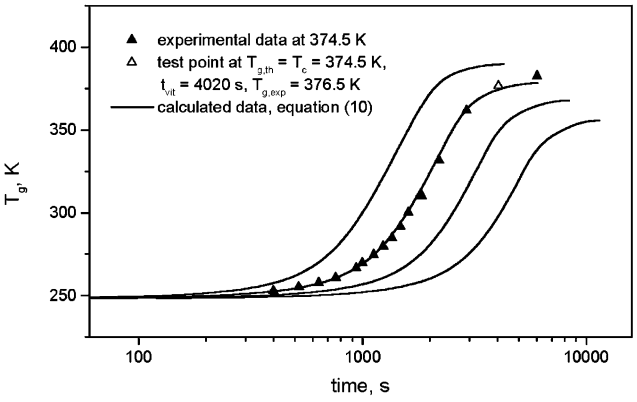

Fig. 8. Superposition plot of the glass transition temperature versus log(time) scale of DGEBA–*m*PDA reaction.

A typical plot of $\dot{r}$ versus α of the reaction of DGEBA with *m*PDA at 374.5 K is shown in Fig. 9. As one can see, this plot is a straight line in the kinetically controlled region when $n = 1.5$–1.6. The same value of n describes well the experimental data in the whole temperature range from 354.5 to 384.5 K. This finding is in agreement with the results in Table 3.

The rate constants of the reaction between DGEBA and *m*PDA is possible to determine by assuming $n = 1.5$ and applying the analytical solution of Eq. (8) [9], viz.

$$Kt = g(\beta) = \frac{2}{b^2}\left(\frac{1}{\beta} - 1\right) + \frac{1}{b^3}\ln\frac{b-\beta}{b+\beta}\frac{b+1}{b-1} \qquad (12)$$

where $\beta = (1-\alpha)^{1/2}$; and $b = (B+1)^{1/2}$.

As a consequence, the kinetic analysis of the data can be performed using both differential and integral single DSC curve methods.

The analysis of the original and α_0-corrected integral data

Table 5
The E_{ap} values calculated using different apparent log(A_{ch}) Arrhenius plot methods

Data type	E_{ap} (kJ mol^{-1})				
	Characteristic variable at a fixed event or degree of conversion, A_{ch}				
	$(d\alpha/dt)_{0.5}$ (s^{-1})	$(d\alpha/dt)_p$ (s^{-1})	t_p (s)	t_v (s)	A_T (364.5 K)
Original data	52.4 ± 0.4	53.2 ± 0.4	58.5 ± 1.8	–	57.7 ± 1.4
α_0-corrected data	52.1 ± 0.4	52.6 ± 0.2	54.8 ± 0.6	54.2 ± 1.0	53.5 ± 0.1

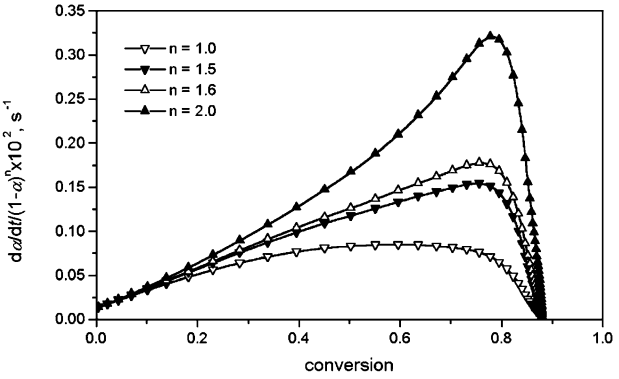

Fig. 9. Dependence of the reduced reaction rate versus the degree of conversion of DGEBA–*m*PDA reaction at different values of the power exponent—see Eq. (11).

has been carried out by varying the value of B until the right hand side term of Eq. (12) becomes a straight line. The best fit values of B and K allow to calculate K'. The rate constants measured in the investigated temperature range and the kinetic parameters evaluated in the kinetically controlled region are given in Table 6.

The autocatalytic rate constant K does not depend of the data type in contrast to K' and B. Its activation energy is perfectly consistent with E_a measured under programmed temperature conditions [9]. It is again evident that α_0-corrected data yield better results.

The best fit values of B and K were found within ± 1 and $\pm 1.3\%$, whereas the fitting error of K at a fixed value of B was less than 1%. The experimental variance of t_0 and K' cause considerably higher errors related to the rate constant K, viz. ± 4 and $\pm 5\%$, respectively. Therefore, the kinetic data derived using Eq. (12) are reliable but their reproducibility depends on some experimental factors.

It is noteworthy that the autocatalytic rate constant for DGEBA–*m*PDA reaction at 364.5 K in Table 6 is of the same order of magnitude as those measured by Aspin et al. for phenyl glycidyl ether–*m*PDA reaction at 363 K [24].

The routine analysis of the α_0-corrected data has been also carried out following the plot of $\dot{r}$ versus α. It is a straight line in the kinetically controlled region if $n = 1.6$. If $n = 1.5$, then the fitting errors referred to K and K' increases more than twice. The rate constants found at different T_c according to Eq. (11) and the calculated kinetic parameters are given in Table 7.

The comparison of the results in Tables 6 and 7 implies that the integral fit yields more reliable data although the overall reaction order seems to exceed slightly 2.5. Hence, the kinetic data derived using the integral method will be further discussed.

3.4. Modeling of the reaction and comparison between the model and the experiment

As previously stated [9], the solution of the direct kinetic

Table 6
Rate constants and kinetic parameters of the DGEBA–*m*PDA reaction calculated according to Eq. (12) and subsequent Arrhenius plot of K_i versus $1/T_c$

Rate constants	Temperature (K)				Kinetic parameters	
	354.5	364.5	374.5	384.5	$\log(K_0)$ (s^{-1})	E_a (kJ mol^{-1})
$K \times 10^3$ (s^{-1} [a])	0.875	1.385	2.152	3.293	4.316 ± 0.021	50.06 ± 0.25
$K' \times 10^3$ (s^{-1} [a])	0.0407	0.0706	0.1291	0.2453	5.587 ± 0.258	67.8 ± 2.8
$B = K'/K$ [a]	0.0465	0.0510	0.0600	0.0745	–	–
$K \times 10^3$ (s^{-1} [b])	0.875	1.385	2.163	3.348	4.405 ± 0.039	50.67 ± 0.55
$K' \times 10^3$ (s^{-1} [b])	0.0407	0.0706	0.1190	0.1959	4.354 ± 0.007	59.36 ± 0.08
$B = K'/K$ [b]	0.0465	0.0510	0.0550	0.0585	–	–

[a] Original experimental data.
[b] α_0-corrected data.

Table 7
Rate constants and kinetic parameters of the DGEBA–*m*PDA reaction calculated according to Eq. (11) and subsequent Arrhenius plot of K_i versus $1/T_c$

Rate constants	Temperature (K)				Kinetic parameters	
	354.5	364.5	374.5	384.5	$\log(K_0)$ (s^{-1})	E_a (kJ mol^{-1})
$K \times 10^3$ (s^{-1} [a])	0.818	1.302	1.980	3.014	4.148 ± 0.030	49.1 ± 0.36
$K' \times 10^3$ (s^{-1} [a])	0.0511	0.0865	0.1608	0.2731	5.155 ± 0.168	64.0 ± 1.9
$B = K'/K$ [a]	0.0624	0.0664	0.0812	0.0906	–	–
$K \times 10^3$ (s^{-1} [b])	0.894	1.443	2.233	3.480	4.489 ± 0.064	51.16 ± 0.45
$K' \times 10^3$ (s^{-1} [b])	0.0452	0.0740	0.1350	0.2142	4.444 ± 0.291	59.7 ± 2.0
$B = K'/K$ [b]	0.0505	0.0513	0.0605	0.0616	–	–

[a] α_0-corrected data, $n = 1.5$.
[b] α_0-corrected data, $n = 1.6$.

problem is the best way to test the reliability of the kinetic parameters. Numerical modeling of different types of chemical reactions either at constant temperature or linear programmed mode is involved in our self developed software for this purpose. It is not necessary in isothermal regime, however, since the velocity equations of DGEBA–*m*PDA reaction have analytical solutions — see Eqs. (12) and (7). This fact enables us to calculate the time scale with respect to α at any T_c applying the integrated form of the following evaluated velocity equations:

$$\frac{d\alpha}{dt} = 2.541 \times 10^4 \exp\left(-\frac{50.67\ \text{kJ mol}^{-1}}{RT}\right) \times \left[0.889 \exp\left(-\frac{8.69\ \text{kJ mol}^{-1}}{RT}\right) + \alpha\right](1-\alpha)^{3/2}\ \text{s}^{-1} \quad (13)$$

and

$$\frac{d\alpha}{dt} = \frac{d\alpha}{dT}\frac{dT}{dt} = 3.130 \times 10^4 \exp\left(-\frac{50.50\ \text{kJ mol}^{-1}}{RT}\right) \times (0.025 + \alpha)(1-\alpha)^2\ \text{s}^{-1} \quad (14)$$

If $B = \text{const}$, then the temperature scale in scanning mode is also possible to calculate using the evaluated form of Eqs. (7) or (12) and the approximate solution of the Doyle's temperature integral. This type of analysis has been performed by Nam and Seferis [25] whose approach, concerning the kinetics of PEEK decomposition, is quite similar to ours. The general case, such as the one expressed with Eq. (13), requires numerical methods to predict the reaction behavior in programmed temperature mode.

Fig. 10 represents the accuracy test of the kinetic parameters in Eq. (13) at different T_c. Perfect agreement between the model and the experiment is observed. The diffusion controlled region is distinctly evident in the figure, as well. The results indicate that the inverse problem of the diffusion controlled kinetics, which is of a special interest in our future research activities, can be reliably solved at $T_c \leq 374.5$ K.

Fig. 11(a) shows the comparison between the experiment at 354.5 K and the data, calculated according to Eqs. (13) and (14), respectively, whereas Fig. 11(b) demonstrates the comparison of the two model predicted data within the investigated temperature range. As one can establish, Eq. (14) describes sufficiently well the initial stage of the isothermal curves ($\alpha = 0$–0.4) where the epoxy–primary amine reaction predominates. The isothermal and non-isothermal model simulated data disagree if $\alpha \geq 0.4$. Taking into account this finding, the experimental data were fitted (within the mentioned α range) to the following

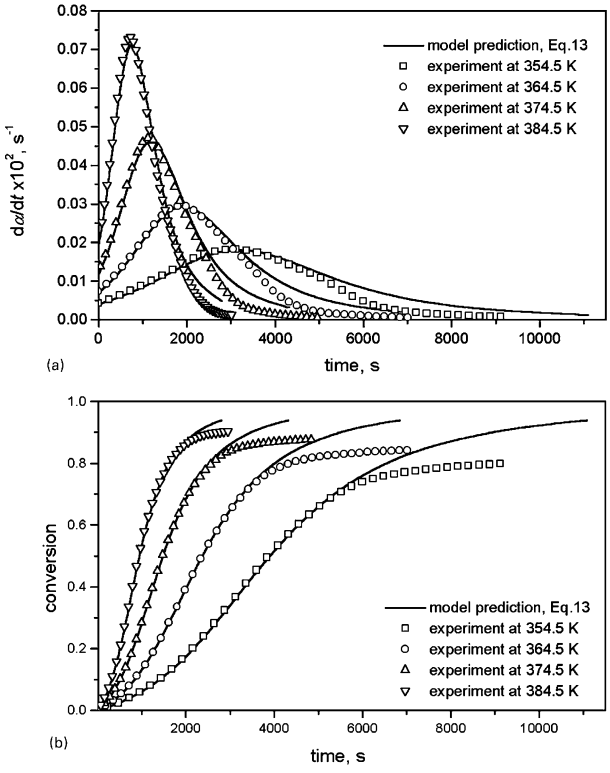

Fig. 10. Comparison of experimental and model predicted data of DGEBA–*m*PDA reaction.

three molecular autocatalytic velocity equation:

$$\frac{d\alpha}{dt} = 3.401 \times 10^4 \exp\left(-\frac{51.20\ \text{kJ mol}^{-1}}{RT}\right) \times \left[0.482 \exp\left(-\frac{7.25\ \text{kJ mol}^{-1}}{RT}\right) + \alpha\right](1-\alpha)^2\ \text{s}^{-1} \quad (15)$$

The test of Eqs. (13) and (15) under programmed temperature conditions (or comparison between the non-isothermal and isothermal DSC kinetics in an inverse order) is demonstrated in Table 8. The results lead to quite unexpected conclusions: (i) the test of the velocity equation that perfectly describes the isothermal data fails in programmed temperature mode; and (ii) the non-isothermal kinetics correlating satisfactorily to the kinetics of the epoxy–primary amine reaction seems to be a more reliable DSC technique. This statement cannot be considered as an exactly reasonable one, as is commented below.

3.5. Discussions

In recent years the interest concerning the kinetics of the epoxy–amine reactions has grown up again in two progressive research areas. The first one relates to the nanoparticles reinforcement of the epoxy composites [26,27]. The second one promotes the investigation of different modified epoxy

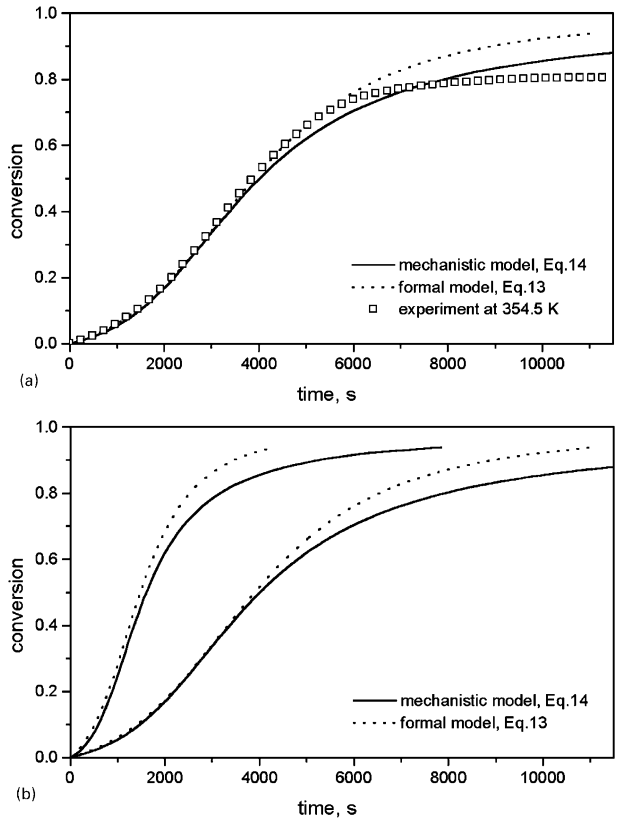

Fig. 11. (a) Comparison of the experiment at 354.5 K and the two model predicted data of DGEBA–*m*PDA reaction. (b) Comparison of two model predicted data of DGEBA–*m*PDA reaction at 354.5 and 374.5 K.

formulations: liquid crystalline polymers and blends [28,29]; low or high modulus polymer toughened semi-IPN [30–36], and full-IPN [36,37]. The backgrounds of the driving force of the phase separating process [38] and the experimental and theoretical origin of the reaction induced phase separation mechanism, are also extensively developed [39,40].

The DSC studies of these materials appear to have important application. The non-isothermal kinetics permits to estimate rapidly the activity of the fillers and the dilution effect of the polymer additives. On the other hand, the curing prehistory controls the phase separating process and the structure of the material. It is noteworthy that the phase separation process also influences the chemical reaction [41]. Hence, a sophisticated velocity equation (or a set of differential equations) that might describe the kinetic data obtained at either constant temperature or linear programmed mode has to be derived.

The results extracted in the four preceding subsections concerning the comparative DSC kinetics of DGEBA–*m*PDA reaction can be summarized, as follows.

1. Based on the analysis at the peak maximum of the DSC curves, it has been established that: (i) the overall reaction order in the investigated temperature range seems to be 2.5 rather than 3; (ii) the monomer mixture is partially reacted during the instrument equilibration at $T_c \geq 374.5$ K.
2. Applying the Arrhenius plot of different characteristic variables and a multiple shift of the DSC curves, the apparent activation energy has been determined within the limits: $E_{ap} = 52.1$–54.8 kJ mol^{-1}. As is seen, the E_{ap} values measured at either constant temperature or linear programmed mode nearly correspond to each other, especially if the conversion at the beginning of the isothermal scans has been taken into account.
3. The velocity equation has been evaluated using both differential and integral single DSC curve methods. The comparison of the results has inferred that the integral fit yields more reliable data although the overall reaction order seems to exceed slightly 2.5. The activation energy of the autocatalytic rate constant determined at constant temperature mode, $E_{a,i} = 50.67$ kJ mol^{-1}, has been found in close agreement with the one obtained in non-isothermal regime, $E_{a,n} = 50.50$ kJ mol^{-1}.
4. The reaction modeling has shown that the velocity

Table 8
Comparison between the model predicted Eqs. (13) and (15), and experimentally measured characteristics at T_p [9] of the DGEBA–*m*PDA reaction under programmed temperature conditions

dT/dt (K min^{-1})	T_p (K)	$(d\alpha/dT)_p$ (K^{-1})	α_p	T_i (K)	T_f (K)	α_f
	Experimental curves [9]					
10	432.9	0.02195	0.4590	343	568	1.000
5.0	414.7	0.02390	0.4565	328	553	1.000
2.5	398.6	0.02640	0.4530	313	538	1.000
	Computer simulated curves Eq. (13)					
10	432.9	0.02340	0.5195	318	533	0.999
5.0	415.6	0.02580	0.5195	313	503	0.999
2.5	399.5	0.02840	0.5190	308	483	0.999
	Computer simulated curves Eq. (15)					
10	430.9	0.01970	0.4525	333	568	0.994
5.0	413.8	0.02175	0.4515	323	553	0.996
2.5	398.0	0.02395	0.4505	318	538	0.997

equation, perfectly fitting the isothermal experiments, fails in programmed temperature mode, and vice versa. On the contrary, the approximated velocity equation of the epoxy–primary amine reaction seems to predict more correctly its non-isothermal behavior.

The discrepancy between the two DSC techniques does not necessary mean that one of them is artificial. The DSC kinetics of the epoxy–amine reaction has a complicated nature and it needs to be carefully analyzed. There are three groups of reasons that are expected to affect the DSC kinetics: physical chemical, methodological, and mechanistic. The mechanistic factors will be only discussed in the present study, although some methodological and physical chemical ones have to be also taken into account.

The deviation of DGEBA–*m*PDA kinetics from the overall model of Horie et al. might be attributed either to the mechanistic scheme of the reaction or to its mathematical description, see Eqs. (1)–(4).

Several comprehensive articles and reviews subjected to the mechanism of the epoxy-amine reaction, as well as to the deviation from the overall three molecular autocatalytic model, are found in literature [3,7,8,12,42,43]. The excellent mechanistic analysis performed in three of them [7,8,42] requires special caution.

Cole [7] extended the model description of the epoxy-amine kinetics explicitly including the etherification reaction. Cole also pointed out that etherification might become significant in epoxy excess and at rather high curing temperatures. As one can establish, the speed of the hydroxyl addition should be negligible compared to the amine addition, which arises from the experimental conditions in the study of DGEBA–*m*PDA reaction.

Mijovic et al. [8] introduced the so called weighing factors expressing the relative driving force of a given reaction path among the competitive ones. Xu et al. [42] argued that the determination of the weighing factors, proposed by Mijovic et al., was rather arbitrary and the application of their model was greatly limited. Xu et al. determined the autocatalytic rate constant parameters assuming two alternative (but not simultaneous) initiation paths, although they also pointed out that it was still not possible to distinguish between them. In our opinion, the weighing coefficients should present unless the elemental rate constants are calculated based on the mass balance equations [7]. Their meaning consists in predicting a complex reaction behavior (governed by more than one driving mechanisms) whose mathematical expression can only be suggested.

In another work, Mijovic et al. [44] proposed a higher value of the power exponent regarding the hydroxyl groups. Although it might explain the deviation of the experiment from the model of Horie et al., the above cited mechanistic studies [8,42] do not directly support this assumption. Hence, the initiation path cannot be related to the present work. As is expected, the dimensionless rearrangement is simplified to identical equations [42].

The mechanistic study of the DGEBA–*m*PDA reaction allows to test another possibility causing the aforementioned discrepancy. It is usually referred to as a transfer of the rate determining step [3,22,42,43]. The mathematical form of this hypothesis ($k^{i-1} \ll k^i$ or $k^i \ll k^{i-1}$) infers that competitive mechanisms are expected to occur in a given temperature range. This idea seems to agree with our experiment although it is hardly to accept that different transition state complexes should overcome an equal energy barrier.

Eqs. (2a–e) or (3a–c) exhibit the effect of the secondary to primary amine reactivity ratio that is also known as kinetic substitution effect (KSE). The analysis of the literature [8,43] shows quite controversial data regarding the reactivity ratio, but negative KSE (or less reactive secondary amines) seems to be a more probable phenomenon. It can be ascribed to the steric hindrances neighboring the secondary amines formed during the reaction of the primary ones. The formal DSC kinetics of DGEBA–*m*PDA reaction was found out either to corroborate the three molecular autocatalytic equation [11,12] or to obey a lower order model [10,13], thus indicating inconstant KSE. From a mechanistic point of view, a lower than three value of the overall reaction order corresponds to positive KSE. According to the literature, in the system chosen there must be little steric influence on the reactivity of the amine hydrogens [8,43] in contrast to our further calculations. On the other hand, the inconstancy concerning the secondary to primary amine reactivity ratio is impossible from a thermodynamic point of view.

In order to explain this anomaly we have made an attempt to derive a modified kinetic model [45]. The main advantage of this model consists in the fact that it accounts for both the reactivity ratio and the solubility of the reaction components. As a first step we have solved the two boundary cases, showing that partial compatibility in the epoxy–amine system might significantly affect the course of the reaction. Moreover, it alternates the highly positive KSE of the DGEBA–*m*PDA reaction, viz. $r = 2.1$ (or $r' = 1.05$). The solubility of the components might have either thermodynamic or kinetic nature. The second possibility, that seems to be the case, converts the model into entirely empirical one, but then it should reflect the sample preparation. The effect of the solubility parameter is more significant than the reactivity ratio, although the boundary solubility model appears to behave more likely as the overall model of Horie et al.

We have to point out that the significant rate constant in the above described kinetic model is exactly the same as the one derived following the formal kinetic model, see Eq. (13). Therefore, the former can be applied in the rheokinetic and diffusion controlled kinetic study of DGEBA–*m*PDA reaction. It is especially valid if the solubility model will turn out to be operative.

4. Conclusions

The isothermal kinetic analysis of DGEBA–*m*PDA

reaction was performed applying an approach similar to the one considering the non-isothermal kinetics of the same reaction that was reported in the preceding paper.

Some of the results derived in the present study are in close agreement with those discussed in the previous one, namely: (i) the values of the apparent activation energy measured at either constant temperature or linear programmed mode nearly correspond to each other, especially if the conversion at the beginning of the isothermal scans is taken into account; (ii) the activation energies of the significant rate constant obtained in both DSC modes exactly coincide; and (iii) the ratios of the impurity catalytic to the autocatalytic rate constant are of the same magnitude.

On the other side, the two DSC kinetic techniques indicate a principle discrepancy. The mechanistic-like three molecular velocity equation sufficiently well describes the non-isothermal DSC kinetics, whereas the isothermal kinetics seems to obey an autocatalytic equation whose overall order is 2.5 rather than 3.

The possible mechanistic factors causing the aforementioned discrepancy were analysed. These are: (i) the presence of a competitive (etherification) reaction; (ii) the complex initiation mechanism; (iii) the transfer of the rate determining step; (iv) the secondary to primary reactivity ratio; and (v) the solubility of the components.

The mechanistic analysis did not directly support the first two possibilities, whereas the reactivity ratio was found to be extremely high. The transfer of the rate determining step was assumed as a reason that probably led to the disagreement between the two DSC kinetic techniques. Having in mind the well-known fact (also corroborated in this work) that the initiation rate constant product vanishes during the reaction advance, then the hydroxyl complex formation will determine the rate controlling path. In our opinion, it is difficult to deduce that different transition state complexes should overcome an equal energy barrier. The solubility of the components was also supposed to be a factor causing the deviation between the isothermal and non-isothermal kinetics of the DGEBA–*m*PDA reaction, that might reflect the sample preparation. Moreover, the solubility model appears to behave more likely as the overall model of Horie et al.

Acknowledgements

A part of this study is financial supported by the National Fund ‘Scientific Investigation’ of the Bulgarian Ministry of Education and Science (Contracts X-209/1992 and X-538/1995). The helpful assistance of Dr V. Stoyanov and Mrs E. Krusteva in preparing the manuscript is also gratefully acknowledged.

References

[1] Horie K, Hiura H, Sawada M, Mita I, Kambe H. J Polym Sci 1970;A-8:1357.
[2] Smith IT. Polymer 1961;2:95.
[3] Barton JM. Adv Polym Sci 1985;72:111.
[4] Wise CW, Cook WD, Goodwin AA. Polymer 1997;38:3251.
[5] Abuin SP, Pellin MP, Pazos MP, Lopez-Quentela L. Polymer 1997;38:3795.
[6] Verchere D, Sautereau H, Pascault JP, Riccardi CC, Moschiar SM, Williams RJJ. Macromolecules 1990;23:725.
[7] Cole KC. Macromolecules 1991;24:3093.
[8] Mijovic J, Fishbain A, Wijaya J. Macromolecules 1992;25:979.
[9] Zvetkov VL. Polymer 2001;42:6687.
[10] Kamal MR, Sourour S, Ryan ME. SPE Tech Pap 1973;19:187.
[11] Sourour S, Kamal MR. Thermochim Acta 1976;14:41.
[12] Prime RB. Thermal characterization of polymeric materials. In: Turi EA, editor. New York: Academic Press, 1981. p. 433, Chapter 5.
[13] Scott EP, Zoubier S. Polym Engng Sci 1993;34:1165.
[14] Wisanrakkit G, Gillham JK. J Appl Polym Sci 1990;41:2885.
[15] Simon SL, Gillham JK. J Appl Polym Sci 1992;46:1245.
[16] Girard-Reydet E, Riccardi CC, Sautereau H, Pascault JP. Macromolecules 1995;28:7599.
[17] Nielsen LE. J Macromol Sci Rev Macromol Chem 1969;C3:69.
[18] DiBenedetto AT. J Polym Sci, Polym Phys 1987;25:1949.
[19] Flammersheim HJ, Horhold HH, Bellstedt K, Klee J. Makromol Chem 1983;184:113.
[20] Spacek V, Pouchly J, Biros J. Eur Polym J 1987;23:377.
[21] Abuin SP, Pellin MP, Nunes L. J Appl Polym Sci 1990;41:2155.
[22] Carrozino S, Levita G, Rolla P, Tombari. Polym Engng Sci 1990;30:366.
[23] Abuin SP, Pellin MP, Nunes L, Gandara JS, Losada PP. J Appl Polym Sci 1993;47:533.
[24] Aspin IP, Hamerton I, Howlin BJ, Jones JR, Parker MJ. Surf Coat Int 1998;18:68.
[25] Nam JD, Seferis JC. J Polym Sci, Polym Phys 1992;33:455.
[26] Kornmann X, Lindberg H, Berglund LA. Polymer 2001;42:1303.
[27] Kornmann X, Lindberg H, Berglund LA. Polymer 2001;42:4493.
[28] Mititelu A, Hamaide T, Novat C, Dupuy J, Cascaval CN, Simionescu BC, Navard P. Macromol Chem Phys 2000;201:1209.
[29] Mijovic J, Chen X, Sy JW. Macromolecules 1999;32:5365.
[30] Wise CW, Cook WD, Goodwin AA. Polymer 2000;41:4625.
[31] Girard-Reydet E, Sautereau H, Pascault JP, Kaetes P, Navard P, Thollet G, Vigier G. Polymer 1998;39:2269.
[32] Poncet S, Boiteux G, Pascault JP, Seytre G, Rogozinski J, Kranbuehl D. Polymer 1999;40:6811.
[33] Chen JL, Chang FC. Macromolecules 1999;32:5348.
[34] Jenninger W, Schawe JEK, Alig I. Polymer 2000;41:1577.
[35] Ritzenthaler S, Girard-Reydet E, Pascault JP. Polymer 2000;41:6375.
[36] Jansen BJP, Rastogi S, Meijer HEH, Lemstra PJ. Macromolecules 1999;32:6290.
[37] Dean K, Cook WD, Zipper MD, Burchill P. Polymer 2001;42:1345.
[38] Borrajo J, Riccardi CC, Williams RJJ, Cao ZQ, Pascault JP. Polymer 1995;36:3541.
[39] Williams RJJ, Rozenberg BA, Pascault JP. Adv Polym Sci 1996;128:95.
[40] Maugey J, Van Nuland T, Navar P. Polymer 2001;42:4353.
[41] Bonnet A, Pascault JP, Sautereau H, Taha M, Camrelin Y. Macromolecules 1999;32:8517.
[42] Xu L, Fu JH, Schlup JR. J Am Chem Soc 1994;116:2821.
[43] Rozenberg BA. Adv Polym Sci 1985;75:113.
[44] Mijovic J, Fishbain A, Wijaya J. Macromolecules 1992;25:986.
[45] Zvetkov VL. Macromol Chem Phys 2001, in press.